

SUPPLEMENTARY INFORMATION

Germanium microflower-on-nanostem as a high-performance lithium ion battery electrode

Gwang-Hee Lee^{1,2}, S. Joon Kwon¹, Kyung-Soo Park¹, Jin-Gu Kang¹, Jae-Gwan Park^{1*},
Sungjun Lee², Jae-Chan Kim³, Hyun-Woo Shim³, Dong-Wan Kim^{3*}

¹*Institute for Multi-Convergence of Matter (IMCM), Korea Institute of Science and Technology (KIST), Seoul 136-791, Korea.*

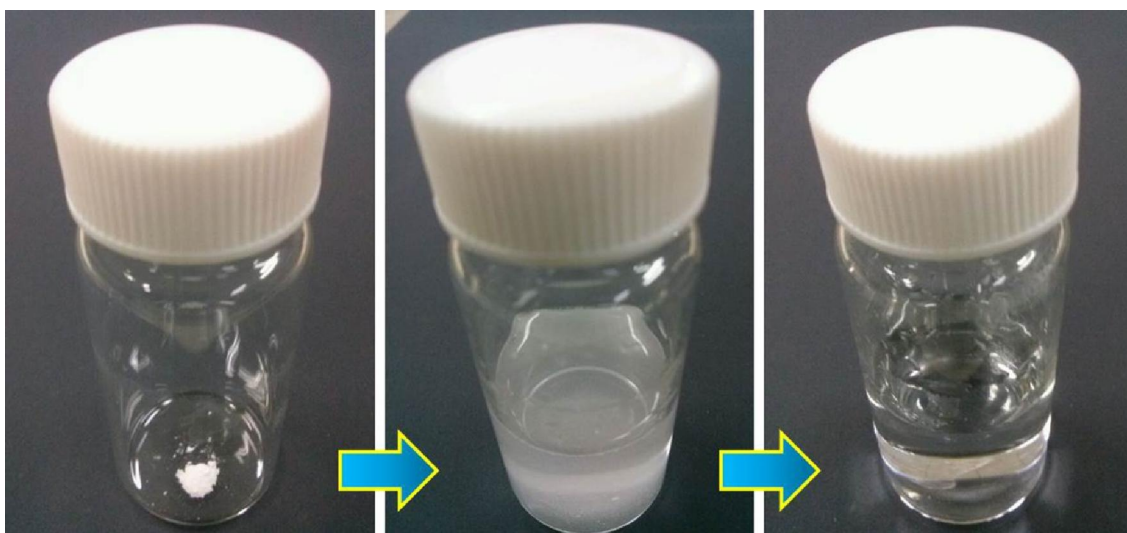
²*Division of Physical Metrology, Korea Research Institute of Standards and Science, Daejeon 305-340, Korea.*

³*School of Civil, Environmental and Architectural Engineering, Korea University, Seoul 136-713, Korea.*

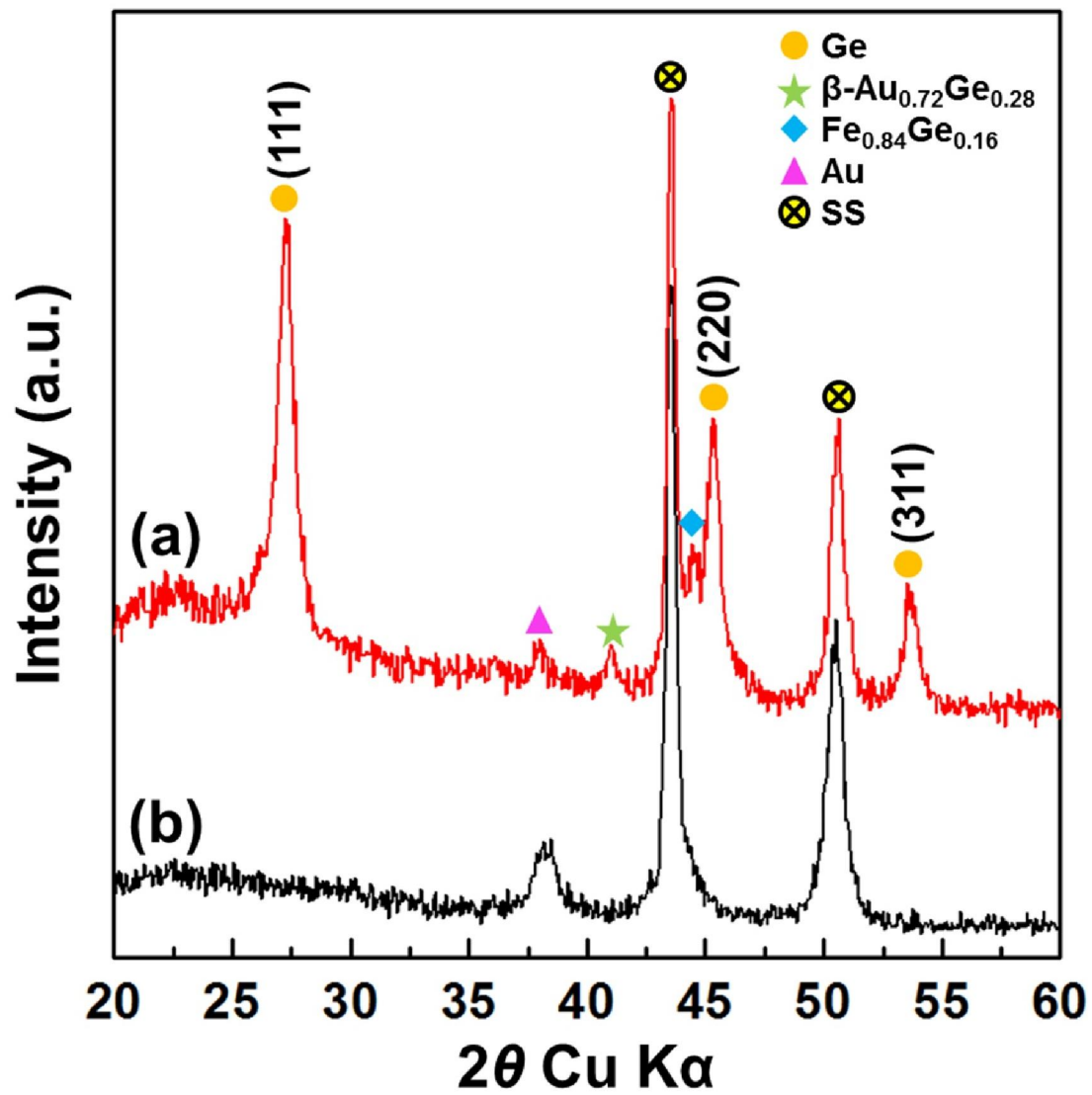
* Corresponding authors.

Tel: +82-2-958-5503, E-mail: jgpark@kist.re.kr (J.-G. Park)

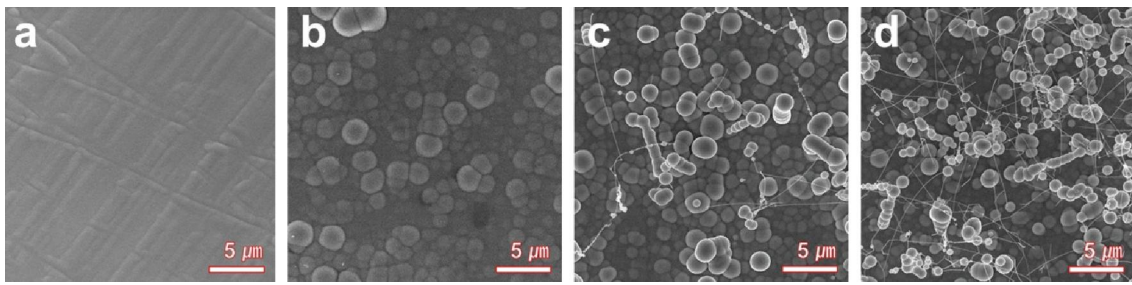
Tel: +82-2-3290-4863, E-mail: dwkim1@korea.ac.kr (D.-W. Kim)



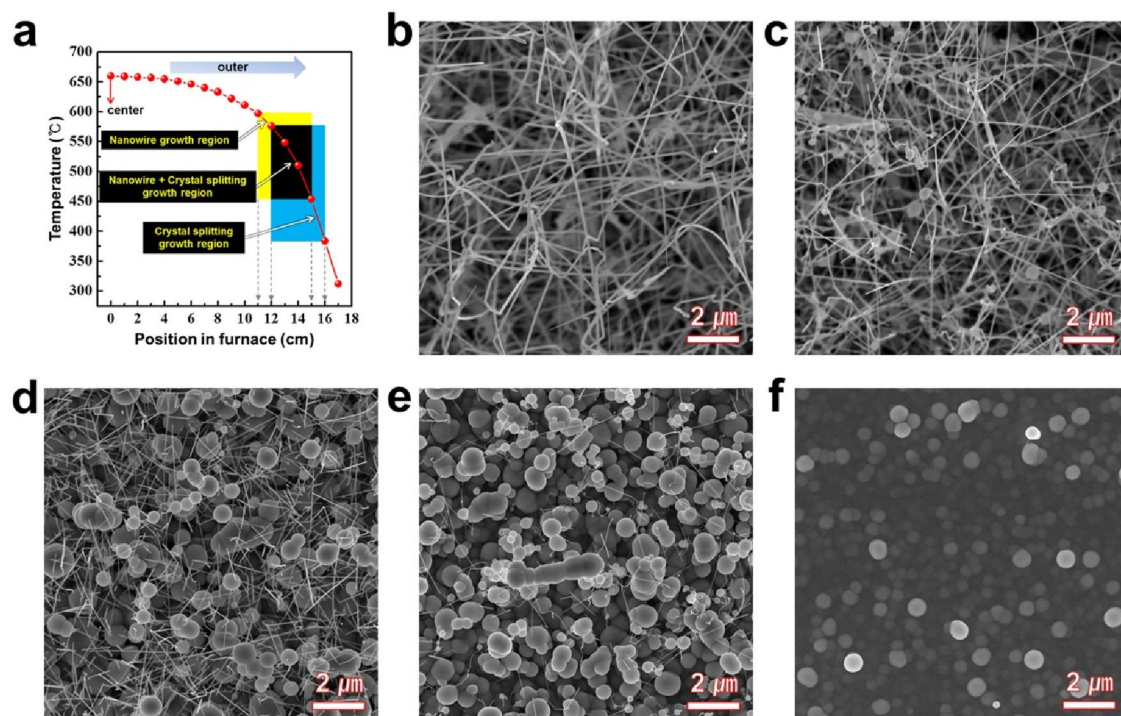
Supplementary Figure S1. Water solubility of amorphous GeO₂. 0.1 g of amorphous GeO₂ (Aldrich, purity 99%) was dispersed in 10 mL distilled water. The amorphous GeO₂ solution was kept at room temperature for 5hr.



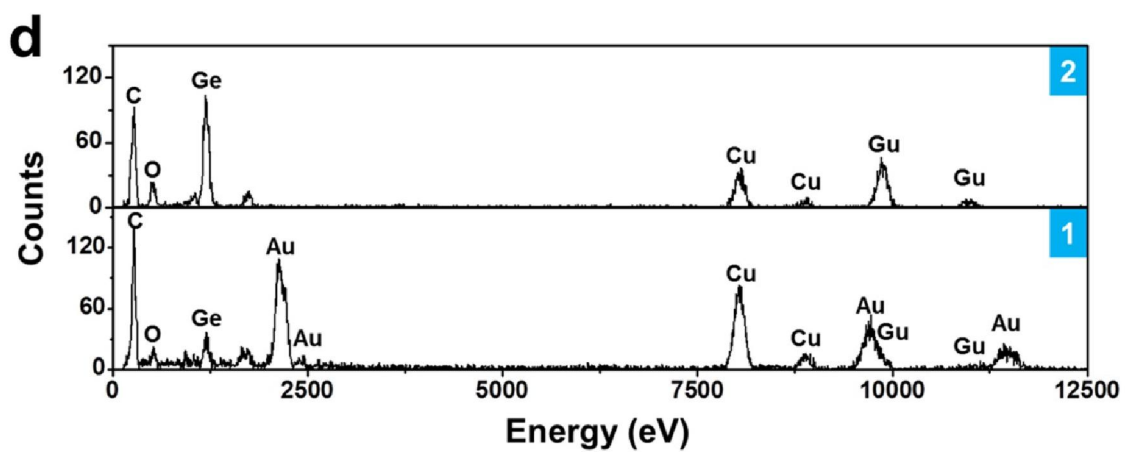
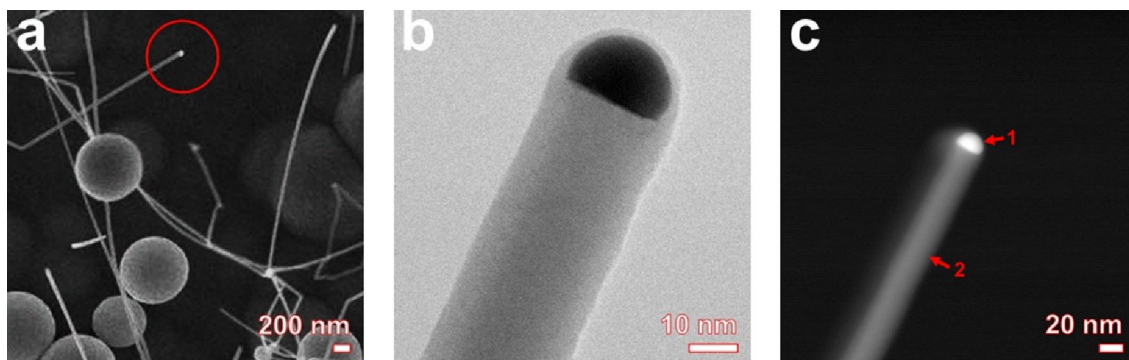
Supplementary Figure S2. XRD patterns of (a) as-synthesized Ge SP-on-NS hybrids grown on a substrate and (b) Au-coated stainless steel substrate.



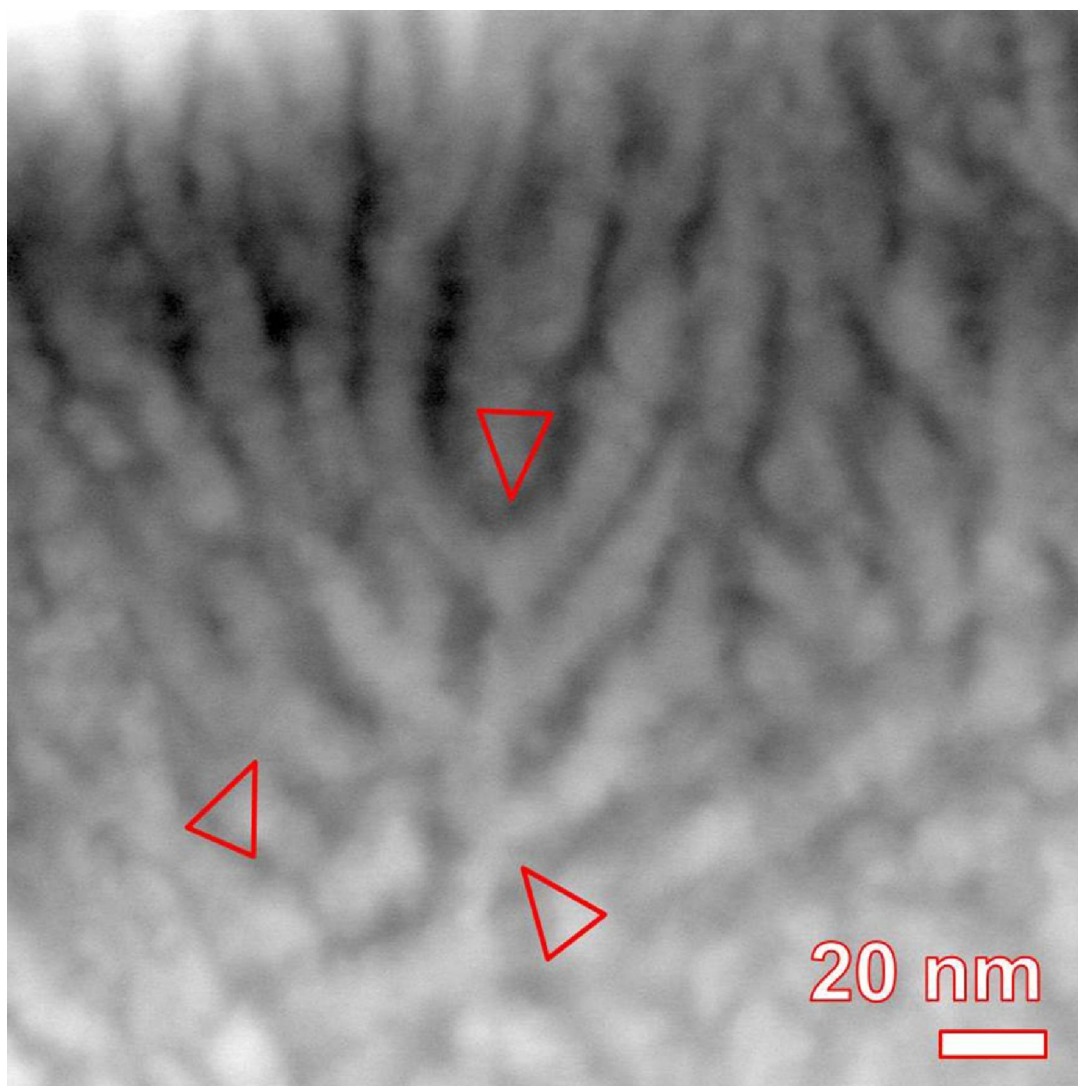
Supplementary Figure S3. FESEM images of Ge SP-on-NS hybrids deposited with (a) 0-nm, (b) 1-nm, (c) 5-nm, and (d) 10-nm Au coating thicknesses.



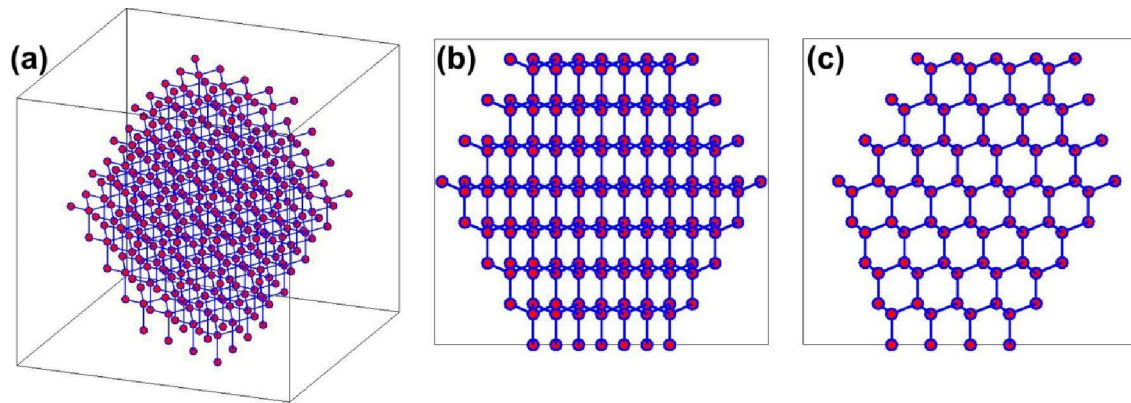
Supplementary Figure S4. (a) Temperature distribution curve from the furnace center. FESEM images of the morphology from the (b) high-temperature zone (11–12 cm, 597–576 °C); (c), (d), (e) medium-temperature zone (12–15 cm, 576–454 °C); and (f) low-temperature zone (15–16 cm, 454–384 °C), respectively. When the growth temperature rapidly decreased, the Ge microspheres are grown through a crystal splitting mechanism. A mixture of microspheres and nanowires is observed in c–e.



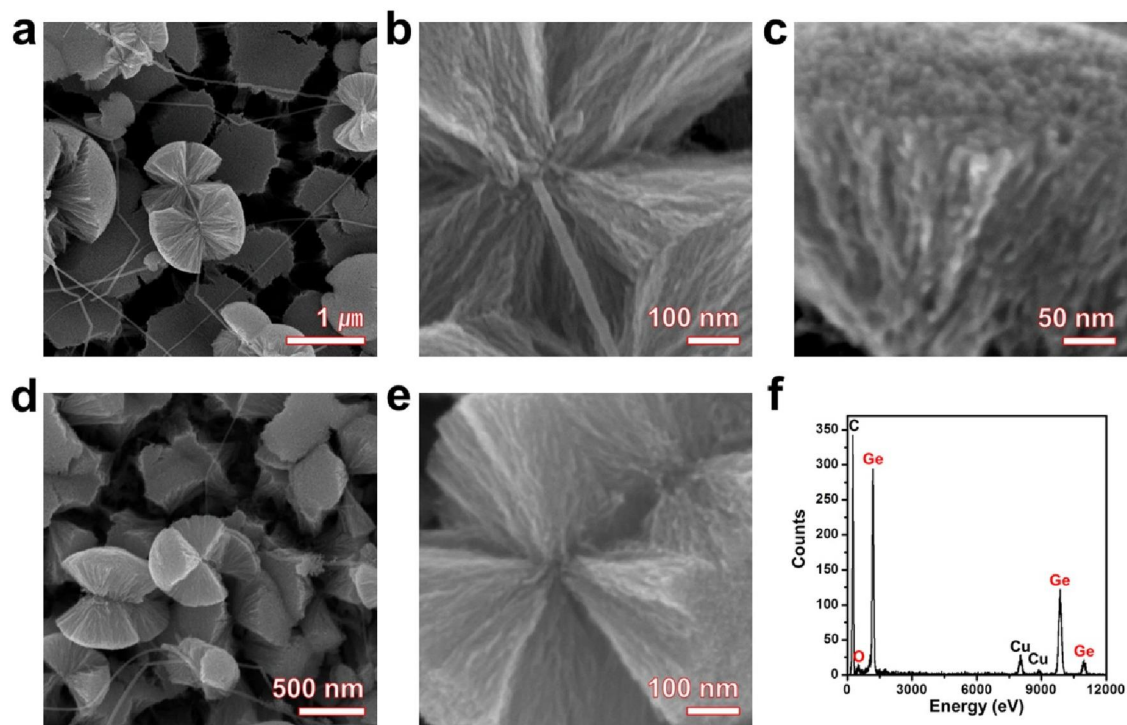
Supplementary Figure S5. (a) FESEM image, (b) typical TEM image, and (c) HAADF STEM image of the tip of Ge nanostems. (d) EDS spectra of the Ge nanostem. Upper section #2 is marked by #2 arrow in (c), and bottom section #1 is marked by #1 arrow in (c).



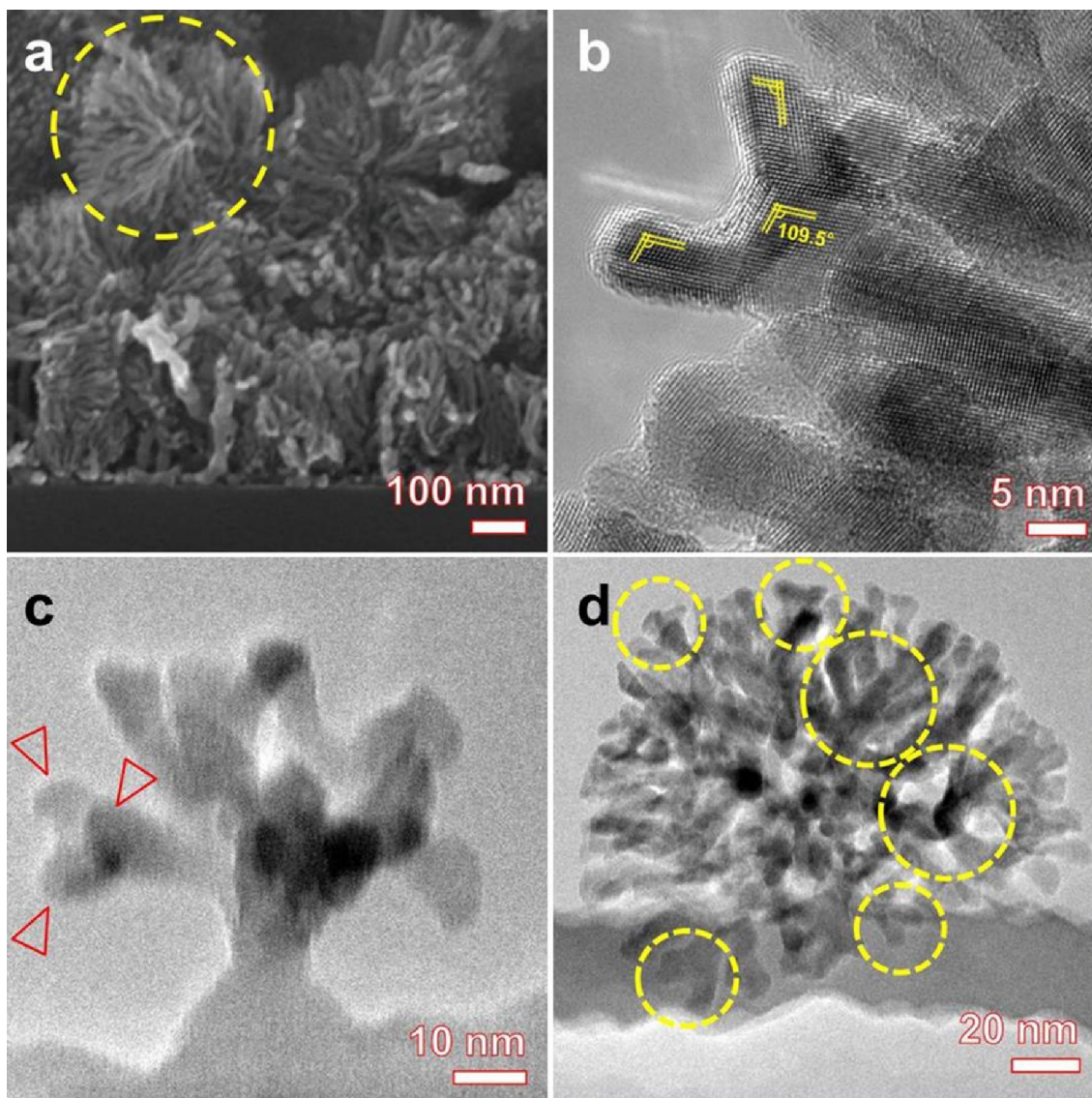
Supplementary Figure S6. HAADF STEM image of the Ge microsphere by FIB to obtain an ultra-thin section. Marked arrows indicate the network structures.



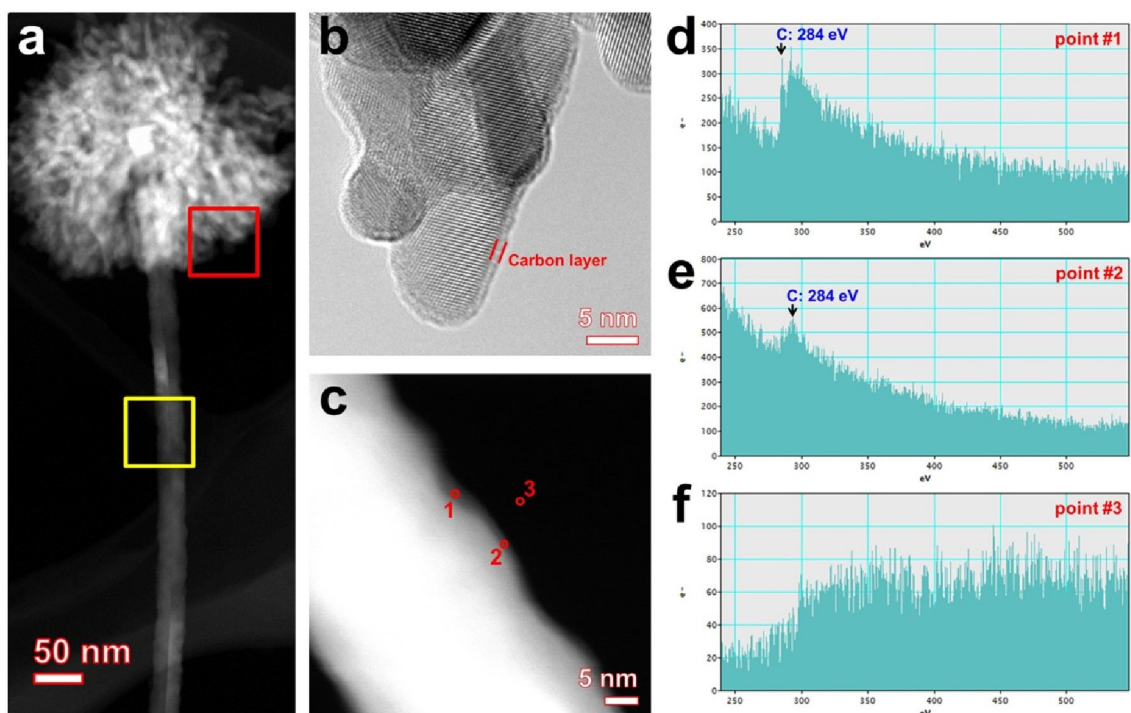
Supplementary Figure S7. (a) A calculated periodic 3-D network model for the Ge nanosphere consisting of 4373 joints and 4372 stems. For the model construction, the tetrahedral replication of stems (blue solid lines) from each of the joints (red spheres) is followed to form a cubic diamond-like periodic structure. Calculated periodic 3-D network models for the Ge nanosphere viewed from the (b) $\langle 1\bar{1}\bar{1} \rangle$ and (c) $\langle 110 \rangle$ directions, respectively.



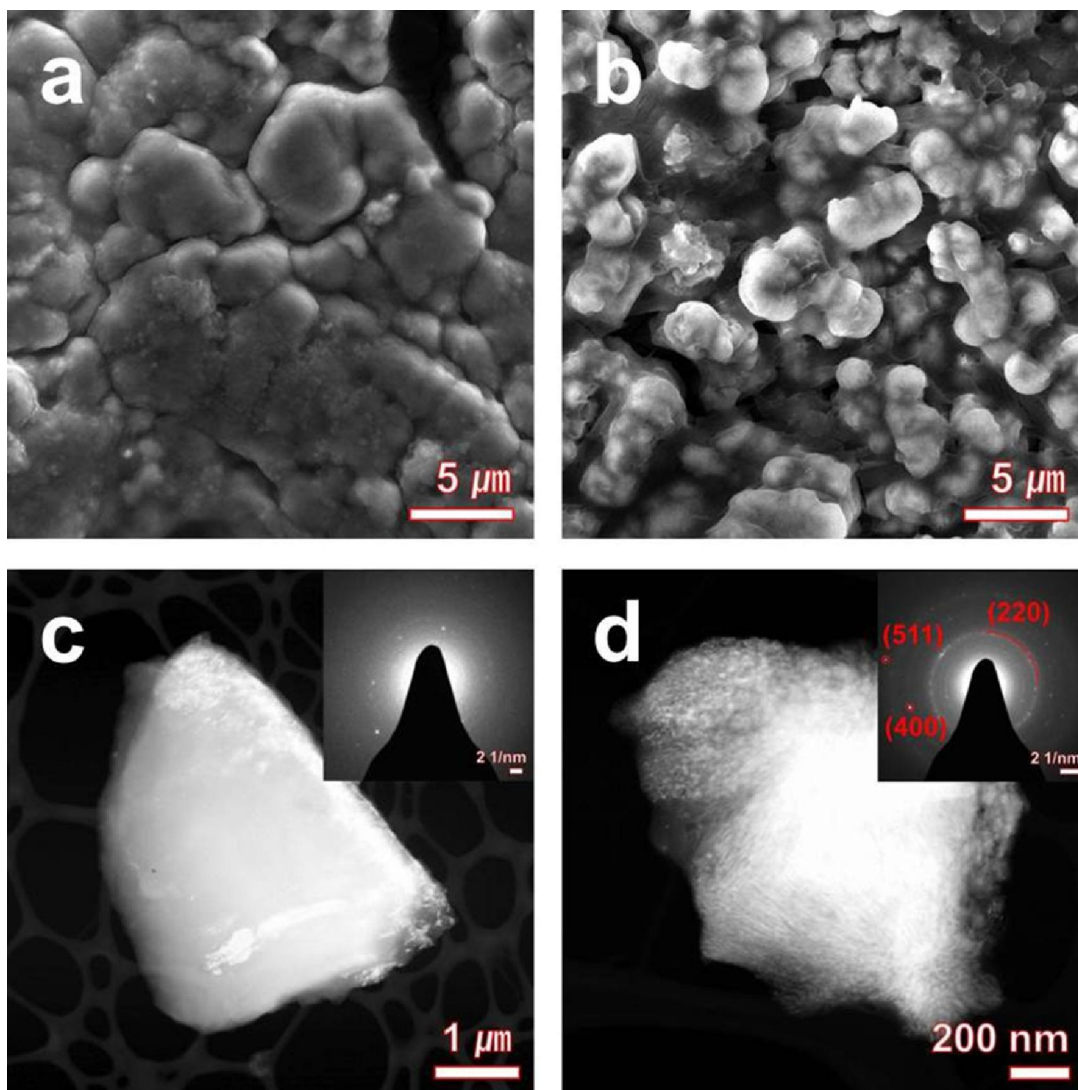
Supplementary Figure S8. (a–e) FESEM images showing the diversity of Ge MF-on-NS hybrids. (f) Representative EDS spectrum of Ge MF-on-NS hybrids.



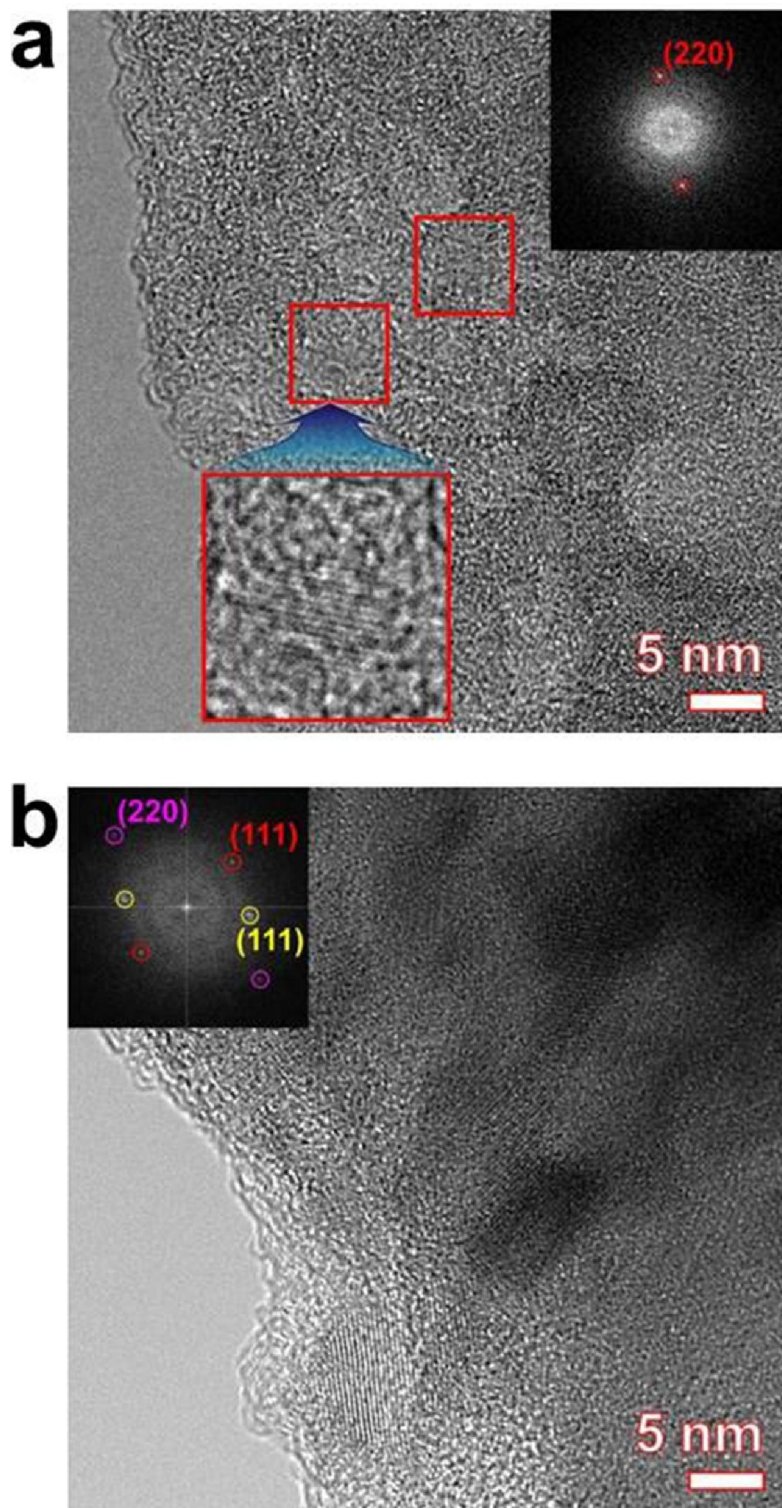
Supplementary Figure S9. (a) FESEM image of the Ge microflowers. (b) HRTEM image of the tetrahedron-prisms unit of the Ge microflowers ($d_{III} = 0.333$ nm). (c,d) TEM images of immature Ge microflowers. Marked arrows indicate the network structure of tetrahedron-prisms unit.



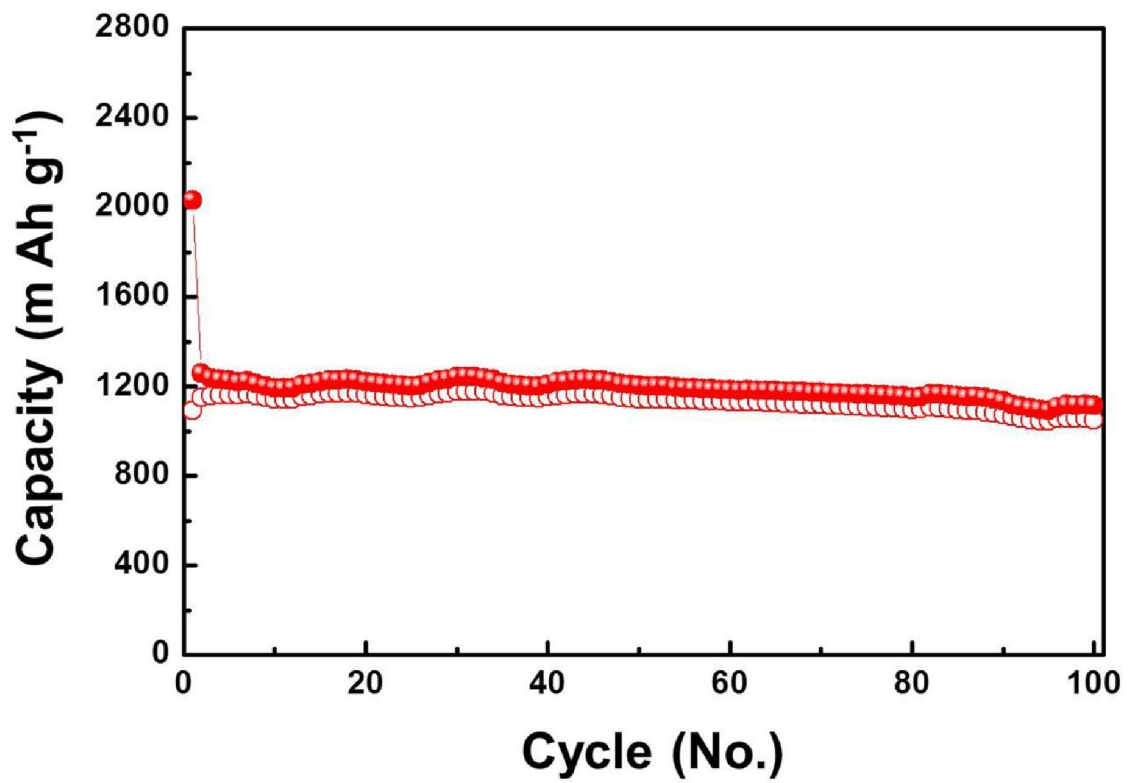
Supplementary Figure S10. (a) HAADF STEM image of an individual Ge MF-on-NS hybrid with a thin carbon sheath. (b) HRTEM image of the dendritic Ge microflower with a thin carbon sheath. (c) HAADF STEM of the Ge nanostem with a thin carbon sheath. (d) EELS spectra with HAADF STEM images obtained from points #1–3, respectively. The EELS spectra of points #1 and #2 indicate the presence of carbon. The amorphous sheath consisted mainly of carbon.



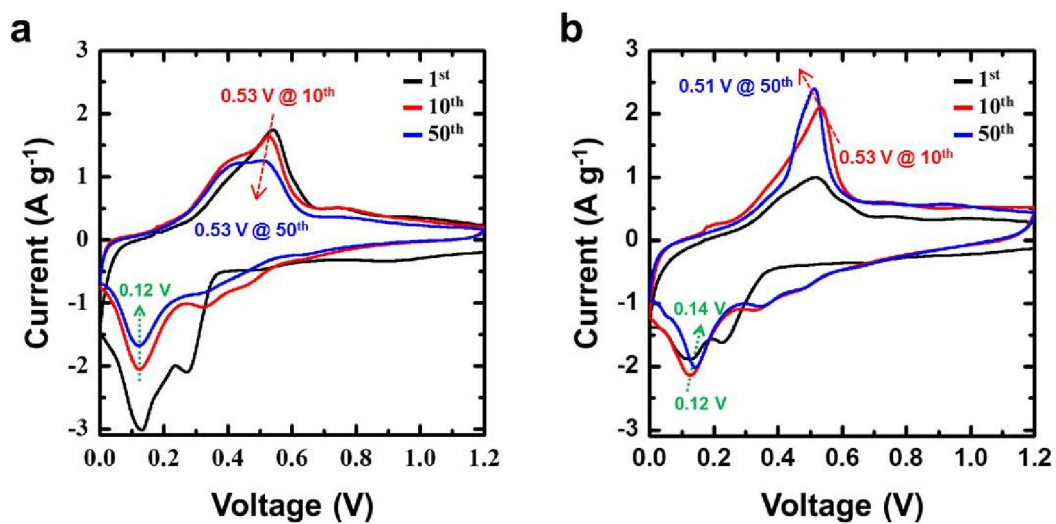
Supplementary Figure S11. Morphology of the bare and carbon-filled Ge MF-on-NS hybrids after 100 charge cycles. Ex situ FESEM images of (a) Ge MF-on-NS hybrids and (b) carbon-filled Ge MF-on-NS hybrids. Ex situ HADDF STEM images of (c) Ge MF-on-NS hybrids and (d) carbon-filled Ge MF-on-NS hybrids. The insets correspond to the SAED patterns.



Supplementary Figure S12. Ex situ HRTEM images of (a) the Ge MF-on-NS hybrids and (b) the carbon-filled Ge MF-on-NS hybrids. The insets are corresponding FFTs.



Supplementary Figure S13. The discharge–charge specific capacity versus the cycle number for the carbon-filled Ge MF-on-NS hybrids electrodes, based on total electrode mass including carbon.



Supplementary Figure S14. Cyclic voltammetry measurement of (a) the Ge MF-on-NS hybrids and (b) the carbon-filled Ge MF-on-NS hybrids at a scanning rate of 0.1 mV s^{-1} during 1st, 2nd, and 50th cycles.